

### 3.1 A neural network to retrieve the mesoscale instantaneous latent heat flux over oceans from SSM/I observations.

Denis Bourras\*, Laurence Eymard†, and W. Timothy Liu\*

\*JPL, NASA, Pasadena, California, USA

†CETP/CNRS/INSU, Vélizy Villacoublay, France

bourras@pacific.jpl.nasa.gov

## 1 Introduction

The turbulent latent and sensible heat fluxes are necessary to study heat budget of the upper ocean or initialize ocean general circulation models. Although monthly means of heat fluxes have been used so far in many of these studies it is now pointed out that high spatial and temporal resolution fluxes are needed to describe correctly the air-sea exchanges (Curry et al., 1999). In order to retrieve the latent heat flux from satellite observations authors mostly use a bulk approximation of the flux whose parameters are derived from different instruments.

$$L_E = \rho L_V C_E U_A (Q_S - Q_A) \quad (1)$$

where  $\rho$  is the density of air,  $L_V$  the vaporization latent heat ( $2.45 \times 10^6 \text{ W.s}$ ), and  $U_A$  the horizontal wind at height  $z_A$ , in  $\text{m.s}^{-1}$ .  $Q_A$  is the specific humidity of the atmosphere at  $z_A$ , in  $\text{g.kg}^{-1}$ , and  $Q_S$  the humidity at surface level.  $C_E$  is the Dalton number which mainly depends on surface boundary layer stability and wind velocity. According to Esbensen et al. (1993) the latent heat flux retrieval error is  $30 \text{ W.m}^{-2}$  at a global scale and on data averaged over 2 months and  $2^\circ$ . At the instantaneous scale however the retrieval error has not been yet assessed accurately because the different spaceborne instrument needed are almost never available simultaneously over the same region. In order to overcome this problem the instantaneous SST maybe replaced by 6 hour or daily averages since except in case of

strong meteorological events this oceanic parameter varies weakly over shorter time scales. On the other hand, a microwave radiometer that measures brightness temperatures ( $T_B$ ) may be used to obtain separately  $U_A$  and  $Q_A$  estimates. This approach may be simplified since it is not efficient to retrieve  $U_A$  and  $Q_A$  from the same  $T_B$  and then use them in equation 1 to obtain the flux. The reason is that the product between  $U_A$  and  $Q_A$  in equation 1 amplifies the retrieval error on each of these parameters (Bourras and Eymard, 1998). It is preferable to relate directly the  $T_B$  to the flux through a multi-linear regression as first demonstrated by Liu (1990). On that subject, Bourras et al. (1999) show that it is more efficient to use the SST and combinations of  $T_B$  instead of single  $T_B$  as inputs of the algorithm. They also point out that a regression is not the most appropriate tool to build a flux retrieval algorithm because it cannot account for the non-linearities between the flux and the input parameters.

In this paper, an approach based on artificial neural networks is proposed and compared to the bulk method on a global data set and 3 local data sets.

## 2 Data sets

### 2.1 Global training data set

The satellite data are the DMSP-SSM/I  $T_B$  which are available at 19, 22, 37 and 85 GHz in both vertical and horizontal polarizations except for the 22 GHz,

available in vertical polarization only. ECMWF analyses at  $1.125^\circ$  are our reference surface data. Tropical Atmosphere Ocean experiment (TAO) buoy data (Hayes et al., 1991) are added to the data set and replace ECMWF parameters when  $Q_A$  is greater than  $19 \text{ g.kg}^{-1}$ . TAO observations are averaged over one hour while the  $T_B$  are averaged over  $\pm 0.3^\circ$  around the buoy locations. The maximum time difference between SSM/I, TAO and ECMWF data is 45 minutes and the SSM/I data are interpolated at the ECMWF resolution. The reference instantaneous flux fields are computed from TAO observations and ECMWF analyses using a bulk iterative algorithm described in Bourras (1999). It is based on bulk coefficient Dupuis et al. (1997) and free convection Fairall et al. (1996) parameterizations. To reject cloudy positions from the data set a liquid water algorithm is used (Gerard et al., 1998). The positions where the integrated water is greater than  $30 \text{ mg.cm}^{-2}$  are deleted from the data set.

To check the consistency of the data set, SSM/I and ECMWF data are compared in terms of  $W$ , which is a standard SSM/I product, and  $U_A$  and  $Q_A$ , as bulk parameters. The satellite estimates are derived from the Goodberlet et al. (1989), Alishouse et al. (1989), and Liu et al. (1984) algorithms. The wind speed rms deviation is  $1.85 \text{ m.s}^{-1}$  and the mean deviation  $0.7 \text{ m.s}^{-1}$ . The rms error on  $W$  is  $0.5 \text{ g.cm}^{-2}$  and the  $Q_A$  error  $2 \text{ g.kg}^{-1}$ .

## 2.2 Local validation data sets

$U_A$ ,  $Q_A$  and bulk  $L_E$  measured inboard R/Vs are compared to SSM/I observations locally. The ship data are averaged over one hour to smooth most of the high frequency (small-scale) variability and the  $T_B$  are averaged over  $\pm 0.3^\circ$ . Data come from the SEMAPHORE (Eymard et al., 1996), CATCH (Eymard et al., 1999) and TOGA/COARE (Webster and Lukas, 1992) experiments which represents very different meteorological conditions.

## 3 Methodology

Fluxes are derived from the Liu and Niiler 1984 method (LN hereafter) and a neural network (NN) approach. In both methods the SST is assumed known and maybe retrieved separately from infrared radiometers on 6 hours or daily averages. The SST used in the following comes from the surface parameters of the data sets described in section 2. For the LN method, the fluxes are derived from Goodberlet, Alishouse and LN algorithms and  $C_E$  is  $1.2 \cdot 10^{-3}$ . The NN model is a multi-layer perceptron which inputs are selected according to the study reported in Appendix A.

## 4 Results

First, the two methods are applied to the global data set and the error is analyzed. Then, the results are validated on the local data sets.

The retrieval error obtained on the global data set is  $54.6 \text{ W.m}^{-2}$ . The LN method systematically produces negative fluxes where  $\Delta Q$  is low because of the retrieval error on  $Q_A$ . The reason is that the  $Q_A : W$  relationship was not intended to work at this timescale. The rms error is  $36.4 \text{ W.m}^{-2}$  when the NN is applied (Figure 1). Spatially, the two methods produce quite similar spatial flux maps although the flux gradients are different. It appears that the LN method produces too large gradients especially at the extreme flux values, which is a consequence of the product between retrieved, thus noisy  $U_A$  and  $Q_A$  in the bulk equation. The NN flux gradients are much weaker than the LN ones and more comparable to the surface data. The latitudinal distribution of the LN flux retrieval error is mainly driven by the  $Q_A$  retrieval error. The  $Q_A$  retrievals are mostly overestimated in the tropical and equatorial latitudes which means that the LN fluxes are underestimated there, while it is the contrary to the higher latitudes. On the other hand the spatial variability of the  $Q_A$  and  $U_A$  error, which is linked to the variability of  $Q_A$  and  $U_A$ , is low in the tropical regions while it is larger over  $30^\circ\text{N}$  mainly in the Atlantic and Pacific Oceans. It points out that the accuracy of the flux algorithm

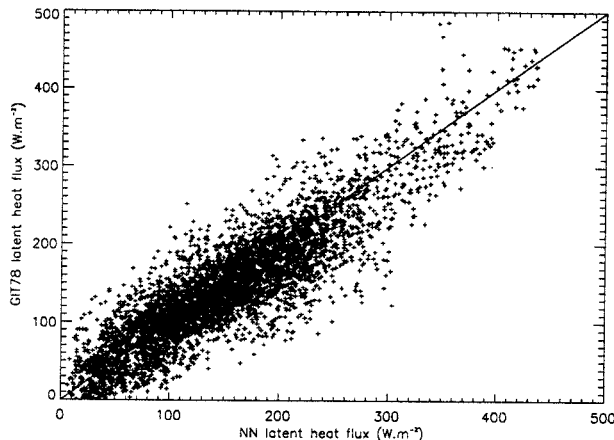


Figure 1: Flux values derived from SSM/I data using the neural network (x-axis), versus ECMWF based fluxes (y-axis) on the global data set.

is very variable in mid latitude regions.

On the SEMAPHORE data set the network gives the lowest rms error,  $26 \text{ W.m}^{-2}$ , but both the LN and the NN fluxes are overestimated: The biases are  $36.3$  and  $40.9 \text{ W.m}^{-2}$  respectively. Those biases are not connected to the  $Q_A$  or  $U_A$  retrieval error but to the surface layer stability since  $C_E$  measured during SEMAPHORE is larger than its value in the corresponding ECMWF analyses. The flux rms error is lower for the NN on CATCH,  $36 \text{ W.m}^{-2}$ . However, although the LN method produces negative fluxes because  $\Delta Q$  is low during CATCH, it works better than the NN at strong fluxes producing no bias beyond  $200 \text{ W.m}^{-2}$ . The combination of humidity to saturation with large liquid water contents in the atmosphere reduces the efficiency of the flux retrieval methods on TOGA/COARE. The flux rms error is  $24.6 \text{ W.m}^{-2}$  for the NN, which is low, but the correlation coefficients are also weak, That is  $0.6$  for LN and  $0.7$  for the NN.

## 5 Conclusion

A new method to retrieve the latent heat flux from satellite data is proposed. It is based on a neural network approach and is designed to retrieve the in-

stantaneous flux at a  $35 \text{ km}$  resolution. Its input parameters are selected according to physical rules and the sensitivity of the network to the latent heat flux is physically explained. In order to train the network a data set based on  $1.125^\circ$  ECMWF analyses and SSM/I  $T_B$  is built. On this data set, the rms deviation between satellite and ECMWF fluxes is  $35 \text{ W.m}^{-2}$  for the NN, that is  $20 \text{ W.m}^{-2}$  less than with the LN method. Nevertheless,  $10 \text{ W.m}^{-2}$  of error must be accounted for  $Q_S$  which is not retrieved in this study. The spatial variability of the error at global scale is larger to the mid latitudes than in the tropics and near the inter-tropical convergence zone. On the other hand, the sensitivity of the satellite to the flux is smaller below  $\pm 30^\circ N$  than at higher latitudes. On three independent local data sets based on data of the SEMAPHORE, CATCH and TOGA-COARE experiment, the flux retrieval error ranges from  $25$  to  $45 \text{ W.m}^{-2}$  for both methods which is consistent with the error found on the global data set.

## A Network input parameters

### A.1 $T_B : L_E$ relationship

The starting point is the microwave radiative transfer equation:

$$T_{B(p)} = (1 - e^{-\tau}) \cdot T_{up} + e^{-\tau} (1 - e_{(p)}) \cdot T_{down} + SST \cdot e_{(p)} \cdot e^{-\tau} \quad (2)$$

in which  $e_p$  is the surface emissivity in polarization  $p$ ,  $\tau$  the atmospheric transmittance,  $T_{up}$  the temperature of the air mass crossed upward by the radiation, and  $T_{down}$  the air temperature for the downward radiation.

Equation 1 is expanded, assuming that  $\alpha = \rho L_V C_E$  is a constant. Then,

$$L_E = \alpha U \cdot Q_S - \alpha U \cdot Q_A \quad (3)$$

Although it is not possible to express  $T_B$  analytically as a function of the full equation 3 it remains feasible for its last term ( $U_A \cdot Q_A$ ) provided that the radiative transfer equation is linearized along with some additional hypotheses. The first approximation

is to consider that all temperatures are equal to a constant  $T_o$  in equation 2 which results in

$$TB_{(p)} = T_o(1 - e^{-2\tau}(1 - e_{(p)})). \quad (4)$$

In a second step we express  $e^{-2\tau}$  and  $e_{(p)}$  as a function of the known parameters  $U_A$  and  $Q_A$ . As we do not consider the effect of cloud liquid water and the influence of the absorption by oxygen is assumed constant ( $\eta_{O_2}$ ),  $\tau$  is a function of the single integrated water vapour content in the form

$$\tau = \frac{W}{W_o}. \quad (5)$$

According to LN,  $W$  is a 5<sup>th</sup> degree polynomial function of  $Q_A$ . The composition of this polynomial by  $e^{-2\tau}$  maybe replaced by a linear function of  $Q_A$  below  $19 \text{ g.kg}^{-1}$  so that the atmospheric absorption term reduces to

$$e^{-2\tau} = \eta_{O_2}(\alpha_1 \cdot Q_A + \beta_1). \quad (6)$$

The empirical model proposed by Hollinger (1971) (private communication) gives a very simple expression of  $e_{(p)}$  as a function of  $U_A$  and SST:

$$e_{\nu(V)} = \frac{\alpha_2}{SST} + \gamma_2 \quad (7)$$

$$e_{\nu(H)} = \frac{\alpha_3}{SST} + \beta_3 \frac{U_A}{SST} + \gamma_3 \quad (8)$$

We only consider the horizontally polarized channels since the others are not sensitive to the wind velocity. Considering that  $SST = T_o$ , the  $T_{BH}$  may be expressed in terms of the product  $U_A \cdot Q_A$ :

$$TB_{(H)} = \eta_{O_2}(\alpha_4 + \beta_4 \cdot Q_A + \gamma_4 \cdot U_A + \delta_4 \cdot U_A \cdot Q_A). \quad (9)$$

According to this equation the horizontally polarized SSM/I channels are sensitive to  $U_A \cdot Q_A$  which is one term of bulk equation (3).

## A.2 Input parameter selection

Equation 3 suggests that we consider two groups of input parameters; one sensitive to the  $U_A \cdot Q_A$  product and another to  $U_A \cdot Q_S$ .

According to the previous section, the sensitivity to  $U_A \cdot Q_A$  is obtained by selecting the  $T_{BH}$ . The contribution of  $U_A$  and  $Q_A$  in equation 9 is removed by adding other input parameters sensitive to each of the terms  $Q_A$  and  $U_A$ : According to equations 4 and 5,  $T_{22V}$  is sensitive to  $Q_A$  since  $W_o$  is low at 22 GHz. Differences between  $T_{22V}$  and another channel close in frequency such as  $T_{19V}$  or  $T_{37V}$  are also used. These combinations reduce the influence of the cloud liquid water on the measurements. The reason is that the sensitivity to liquid water is the same for both channels since they are close in frequency while the sensitivity to  $Q_A$  is different (as the 22V GHz channel is centred on the water vapour ray). Thus, the usable differences are  $T_{22V} - T_{19V}$  and  $T_{22V} - T_{37V}$ .

The inputs sensitive to  $U_A$  are brightness polarization ratios in which the contribution of the atmospheric transmittance cancels out:

$$Pol_{19} = \frac{T_o - T_{19V}}{T_o - T_{19H}} \equiv \frac{1 - e_{19V}}{1 - e_{19H}} \quad (10)$$

$$Pol_{37} = \frac{T_o - T_{37V}}{T_o - T_{37H}} \equiv \frac{1 - e_{37V}}{1 - e_{37H}} \quad (11)$$

Finally,  $Q_S$  and the polarization ratios (equations 7 and 8) are used to obtain sensitivity to  $U_A \cdot Q_S$ .

Eventually, the polarization ratios at 19 and 37 GHz are selected for their sensitivity to  $U_A$  while the 22V channel and the  $T_{22V} - T_{19V}$  and  $T_{22V} - T_{37V}$  differences ensure the sensitivity to  $Q_A$ . These inputs, in combination with  $Q_S$  and the 19H and 37H channels, provide the sensitivity to  $U_A \cdot Q_A$  and  $U_A \cdot Q_S$ , that is to  $L_E$ .

## References

- [1] Alishouse, J. C., S. Snyder, J. Vongsathorn, and R. R. Ferraro, 1990, Determination of oceanic total precipitable water from the SSM/I, IEEE Trans. Geosci. Remote Sens., 28, pp. 811-822.
- [2] Bourras, D., and L. Eymard, 1998, Direct retrieval of the surface latent heat flux from satellite data; comparison to Liu et al [1984] method on data of the SEMAPHORE experiment, Proc. 9th conference on Satellite Meteorology and Oceanography, 1,, AMS, France, pp. 278-282.

- [3] Bourras, D., L. Eymard, and C. Thomas, 1999, A comparison of the errors associated with the retrieval of the latent heat flux from individual SSM/I measurements, in *Microwave radiometry and remote sensing of the Earth's surface and Atmosphere*, edited by P. Pampaloni and S. Paloscia (VSP publisher), pp. 47-56.
- [4] Bourras, D., 1999, Estimation of the latent heat flux over oceans from satellite data, Thesis, 203 pp., Paris VI University, France.
- [5] Curry, J. A., C. A. Clayson, W. B. Rossow, R. Reeder, Y-C. Zhang, P. J. Webster, G. Liu, and R.-S. Sheu, 1999, High resolution Satellite-derived data set of the surface fluxes of heat, freshwater, and momentum for the TOGA COARE IOP, *Bull. Amer. Meteor. Soc.*, 80, 10, pp. 2059-2080.
- [6] Dupuis H., Taylor P. K., Weill A., 1997, Inertial dissipation method applied to derive turbulent fluxes over the ocean during the SOFIA/ASTEX and SEMAPHORE experiments with low to moderate wind speed, *J. Geophys. Res.*, 102, C9, pp. 21115-21129.
- [7] Esbensen, S. K., D. B. Chelton, D. Vickers, and J. Sun, 1993, An analysis of errors in Special Sensor Microwave Imager evaporation estimates over the global oceans, *J. Geophys. Res.*, 98, C4, pp. 7081-7101.
- [8] Eymard, L., et al., 1996, Study of the air-sea interactions at the mesoscale: The SEMAPHORE experiment, *Ann. Geophysicae*, 14, pp. 986-1015.
- [9] Eymard, L., et al., 1999, Surface fluxes in the North Atlantic current during the CATCH/FASTEX experiment, *QJRM*, 125 (561), pp. 3563-3599.
- [10] Fairall, C.W., E.F. Bradley, D.P. Rogers, J.B. Edson, and G.S. Young, 1996, Bulk parameterization of air-sea fluxes for Tropical Ocean-Global Atmosphere/Coupled-Ocean Atmosphere Response Experiment (TOGA-COARE). *J. Geophys. Res.*, 101, pp. 3747-3764.
- [11] Gerard, E., and L. Eymard, 1998, Remote sensing of integrated cloud liquid water : development of algorithms and quality control, *Radio Science*, 33, 2, pp. 433-447.
- [12] Goodberlet, M. A., C. T. Swift, J. C. Wilkerson, 1990, Ocean surface wind speed from the Special Sensor Microwave/Imager (SSM/I), *IEEE Trans. Geosci. Remote Sens.*, 28, 5, pp. 823-828.
- [13] Hayes, S.P., L.J. Mangum, J. Picaut, A. Sumi, and K. Takeuchi, 1991, TOGA-TAO: A moored array for real-time measurements in the tropical Pacific Ocean. *Bull. Am. Meteorol. Soc.*, 72, pp. 339-347.
- [14] Liu, W. T., and P. P. Niiler, 1984, Determination of monthly mean humidity in the atmospheric surface layer over oceans from satellite data, *J. Phys. Oceanogr.*, 14, pp. 1451-1457.
- [15] Liu, W. T., 1990, Remote sensing of surface turbulent heat flux, *Surface Waves and Fluxes*, G. C. Geernaert and W. J. Plant, 2, Kluwer Academic Publishers, pp. 293-309.
- [16] Webster, P. J. and R. Lukas, 1992, TOGA COARE: The Coupled Ocean-Atmosphere Response Experiment. *Bull. Amer. Met. Soc.*, 73, pp. 1377-1416.